

DEPARTMENT OF PHYSICS, UNIVERSITY OF JYVÄSKYLÄ
RESEARCH REPORT No. 7/1998

**PHYSICS, TESTS AND INSTRUMENTATION OF COULOMB
BLOCKADE PRIMARY THERMOMETRY**

**BY
JUHA KAUPPINEN**

Academic Dissertation
for the Degree of
Doctor of Philosophy



Jyväskylä, Finland
August 1998

URN:ISBN:978-951-39-9802-8
ISBN 978-951-39-9802-8 (PDF)
ISSN 0075-465X

Jyväskylän yliopisto, 2023

ISBN 951-39-0283-8
ISSN 0075-465X

DEPARTMENT OF PHYSICS, UNIVERSITY OF JYVÄSKYLÄ
RESEARCH REPORT NO. 7/1998

**PHYSICS, TESTS AND INSTRUMENTATION OF COULOMB
BLOCKADE PRIMARY THERMOMETRY**

**BY
JUHA KAUPPINEN**

Academic Dissertation
for the Degree of
Doctor of Philosophy

To be presented, by permission of the
Faculty of Mathematics and Natural Sciences
of the University of Jyväskylä,
for public examination in Auditorium FYS-1 of the
University of Jyväskylä on August 21, 1998
at 12 o'clock noon



Jyväskylä, Finland
August 1998

Preface

The work reviewed in this thesis has been carried out during the years 1994 - 1998 at the University of Jyväskylä, Department of Physics. I express my best gratitude to my supervisor, Prof. Jukka Pekola, for his efficient guidance. I wish to thank Prof. Mikko Paalanen for his encouragement in the beginning of this work. All the members of our research group are much thanked for pleasant collaboration. I would also like to thank the staff of our Department of Physics. Financial support from the Graduate School of Material Physics, Jenny ja Antti Wihurin säätiö, Suomen Kulttuurirahasto, and the Department of Physics is gratefully acknowledged.

Jyväskylä, August 1998

Juha Kauppinen

Contents

1. Introduction	4
2. Single electronics and Coulomb blockade	4
3. Nanofabrication	6
3.1 Regular methods	6
3.2 Future methods for high temperature applications.....	8
4. Temperature and cryogenic thermometry	9
4.1 Temperature: definition and scales.....	9
4.2 Cryogenic thermometers	11
4.2.1 Gas thermometry.....	12
4.2.2 Vapour pressure thermometry.....	12
4.2.3 Helium melting pressure thermometry.....	13
4.2.4 Acoustic thermometry.....	14
4.2.5 Viscosity thermometry.....	14
4.2.6 Thermoelectricity	15
4.2.7 Resistance thermometry	16
4.2.8 Diode thermometry	18
4.2.9 Capacitance thermometry.....	18
4.2.10 Noise thermometry.....	18
4.2.11 Magnetic thermometry with electronic paramagnets.....	19
4.2.12 Nuclear magnetic thermometry.....	20
4.2.13 Nuclear orientation thermometry	21
4.2.14 CBT thermometry	22
4.3 Summary	24
5. Publications	27
6. The author's contribution.....	30
7. References.....	31

1. Introduction

This thesis presents the development of Coulomb blockade thermometry (CBT), invented at the University of Jyväskylä in 1994 [P1], from an idea to a practical cryogenic primary thermometer. The principles and tests of CBT are reviewed in papers P1 - P8 and P10. A brief discussion on the basics of single electronics and on the fabrication methods of single electron devices will be presented first. The concepts of temperature and temperature scales will be discussed next and an overview of methods for measuring temperature, including CBT, is given. This will be limited to cryogenic temperatures because the purpose is to give an idea of how our own proposal fits in among the present cryogenic thermometers, and to what extent it meets the requirements in low temperature thermometry.

Two alternate signal conditioning units for different applications developed in order to apply CBT in everyday laboratory use are introduced in paper P10. We have shown that the performance of CBT is excellent in a high magnetic field and that the sensors can be produced with reasonably high yield. [P7, P10] CBT has been developed to a level close to a commercial product.

2. Single electronics and Coulomb blockade

Coulomb blockade thermometry is based on the phenomenon of single electron charging. Here we consider general aspects of single electron tunneling. The reader is advised to the papers P1 - P8 and P10 of this thesis to get acquainted with the principles of Coulomb blockade thermometry. A short introduction can be found in the paragraph 4.2.14 of this thesis, too.

Let us first consider two conductors overlapping and separated by a thin insulating layer forming a junction whose capacitance is C (see Fig. 1). From the classical point of view electrons cannot penetrate the insulator, but quantum mechanics allows electrons to pass through the potential barrier with a certain

probability. This event is called electron tunneling and the structure in Fig. 1 depicts a solid state tunnel junction. [1,2]

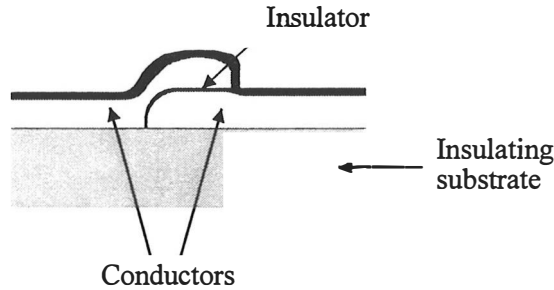


Fig. 1. Two overlapping conductors separated by an insulating layer forming a tunnel junction.

Consider a pair of tunnel junctions with capacitance C connected together and biased by a voltage V . The capacitance of the island between these two junctions to its environment is then $2C$, if we ignore the stray capacitances. Adding one electron to the island increases the energy by an amount $e^2/2C$. If the temperature and the bias voltage are low enough so that $e^2/2C \gg k_B T, eV/2$, electrons cannot get enough energy to tunnel into or from the island in the first approximation. No current flows even at nonzero bias voltage. This phenomenon is called Coulomb blockade.

An energy scale corresponding to such single electron charging effects is thus $E_C \equiv e^2/2C$. If the capacitance of the junction is as small as $C = 10^{-15}$ F, the charging energy is $E_C \approx 10^4$ eV. Another important energy contribution is the thermal energy $k_B T$. If this is much smaller than the charging energy, one can expect single charge effects. For a capacitance $C = 10^{-15}$ F this yields $T \ll 1$ K.

By oxidation of metal one can form insulator layers about 10 \AA thick. According to the basic expression for a parallel plate capacitor we have $C = \epsilon A/d$, where $\epsilon = \epsilon_r \epsilon_0$ is the dielectric constant of the insulator; $\epsilon_0 = 8.85 \times 10^{-12}$ F/m is the permittivity of free space and $\epsilon_r \approx 10$ for the oxide whose thickness is d . A is the overlap area. In order to get $C = 10^{-15}$ F an overlap area of $(100 \text{ nm})^2$ is required. The single-electron

tunneling becomes observable at room temperature if junctions with capacitance being order of 10^{-18} F or area of less than about $(10 \text{ nm})^2$ can be fabricated.

Charge in the double junction system can be controlled, even with a precision of just one electron, by attaching a gate electrode to the structure. Such a device is called a single electron transistor (SET) and it is maybe the most intensively studied configuration of single electronics. The studies of single electron tunneling have been mostly focused on the regime of strong Coulomb blockade, where $E_C \gg k_B T$, whereas our device, CBT, operates in the high temperature limit, where $E_C < k_B T$. The current through tunnel junctions is not prohibited but the current-voltage characteristics are still affected by single electron charging.

3. Nanofabrication

Experimental verification of the theoretical results in single electronics and realisation of the devices call, of course, for methods of fabrication of nanoscale structures. These methods have been intensively studied and developed during the past two decades. The fast development of microlithography started in the early 1970s. At about that time the first applications of electron beam in pattern generation appeared. [3] This enabled the fabrication of devices with feature sizes less than 100 nm, and the experimental research on single electron phenomena, but actually the first realisations appeared only about ten years ago. [4]

3.1 Regular methods

In a lithography process a desired pattern is transferred on a thin layer of material which is sensitive to radiation (light, X-rays, ions, or electrons). This active film, resist, can be selectively removed after the exposure and the structures are generated on the substrate by etching or deposition of other materials.

Optical lithography uses light to expose a thin layer of photoactive polymer material, photoresist, through a mask on a substrate. It is the most widely used method especially in microelectronics industry. The minimum size of the features fabricated

by optical means is limited by the diffraction of light, being dependent on the wavelength of the light used. It is forecasted that linewidths of about 100 nm will be achieved [3] and the present laboratory resolution is not far from that. However, real nanosize structures seem to be beyond the possibilities of optical lithography.

The wavelength of X-rays is in the range of 0.01 – 1.0 nm. This gives a better resolution than that of optical lithography. Structures of 40 nm have been demonstrated, but the method is not widely used probably due to the complexity of such an exposure system. Much less effort has been put on the development of X-ray lithography compared with optical and e-beam lithography.

Electron beam lithography is the main tool in well controlled nanoscale fabrication. By electromagnetic lenses the electron beam can be easily focused to a diameter of few nanometers. The minimum resolution is about 20 nm limited mostly by properties of the resists and electron scatter in the resist and in the substrate. Even though mainly used for research purposes, electron beam lithography has been introduced into industry especially in making masks for optical and X-ray lithography but also in direct fabrication of prototypes and in small volume manufacture.

A focused beam of ions has also been used in lithography, but mainly for ion implantation in doping purposes.

Evaporation and sputtering are standard methods for generating thin films, typically from tens of Ångströms to few micrometers of thickness. Thin layers can also be formed by oxidation, chemical vapour deposition, plasma deposition or epitaxy. A variety of wet and dry etching techniques are used to remove material in order to form structures with dimensions down to nanometer scale. [5]

The fabrication in this work has been carried out using standard electron beam lithography with double layer resist yielding a minimum linewidth of somewhat below 100 nm, and evaporation and room temperature oxidation of aluminium.

3.2 Future methods for high temperature applications

The possible extension of the CBT range to higher temperatures would require a well controlled and reproducible process to fabricate arrays of even smaller tunnel junctions. Taking into account uniformity requirements in CBT fabrication, the present techniques are not applicable for much smaller structures than what we have used so far. Several attempts have been done to extend the operation temperature of single electron devices up to room temperature, which is a natural goal for most applications. Some of those methods are briefly summarised in the following.

Conventional electron beam techniques have been used together with reactive ion etching (RIE) [6], or with ionising beam [7] to fabricate multiple tunnel junctions showing charging effects up to 77 K and above. Electron beam and RIE techniques have been applied in fabricating point contacts on silicon, and the transistor properties were shown to persist to above 77 K. [8,9] Scanning tunneling microscope (STM) has been used to fabricate tunnel junctions showing charging effects at room temperature. [10] The idea was to make nanometer size lines by anodically oxidising a thin metal film by the tiny metal tip of the STM. An atomic force microscope with a similar technique but in a more controllable configuration has been also applied. [11] Memory units operating at room temperature based on SET have been demonstrated using e-beam lithography and RIE together with chemical vapour deposition. [12,13,14] More proposals for new nanofabrication techniques are found e.g. in Ref. 15.

The process control and yield, and the uniformity in fabricating repeated structures in the examples above seem to be still far from the required level e.g., for fabricating tunnel junction arrays for CBT. The critical design parameters and uniformity requirements of CBTs are discussed thoroughly in papers P5 and P10 of this thesis.

4. Temperature and cryogenic thermometry

4.1 Temperature: definition and scales

Temperature determines the direction of heat flow when an object is brought into thermal contact with another one. Heat flows from the object at higher temperature to that at lower temperature. Temperature is thus a property that determines whether or not two bodies in thermal contact with each other are in thermal equilibrium. If thermal equilibrium exists, i.e. no heat flow occurs between the bodies, they are known to be at the same temperature. Further, if two bodies are in thermal equilibrium with a third body they are also in thermal equilibrium with each other. This basic fact enables comparison of the temperatures of two bodies and thus the use of a thermometer. [16,17]

The definition of thermodynamic or absolute temperature can be obtained from a reversible process called a Carnot cycle. It uses two heat reservoirs at different temperatures T_1 and T_2 . The process is represented on a (p, V) diagram in Fig. 1 with gas as a working substance. The cycle consists of four phases: 1. In an isothermal process (AB) at temperature T_1 heat ΔQ_1 is absorbed from the reservoir. 2. An isentropic (= reversible and adiabatic) process (BC) cools the working substance to temperature T_2 . 3. During an isothermal process (CD) at $T = T_2$ heat ΔQ_2 is rejected from the system to the reservoir. 4. An isentropic process (DA) returns the system to its original state. In a reversible cycle the ratio $\Delta Q_2 / \Delta Q_1$ depends only on the temperatures T_1 and T_2 . The absolute temperature scale can be established by requesting that

$$\frac{T_1}{\Delta Q_1} = \frac{T_2}{\Delta Q_2}. \quad (1)$$

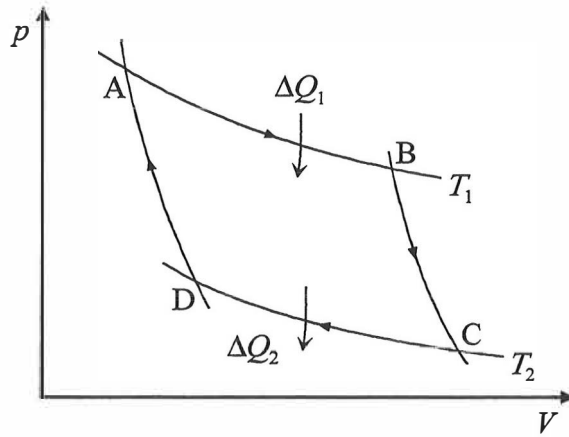


Fig. 1. A Carnot cycle on a (p,V) diagram.

Relation (1), as well as other alternative definitions, give only the ratio of the temperatures; the scaling factor for absolute values of the temperature scale has to be fixed. The most important non-absolute temperature scale in everyday practical use is the one proposed by Celsius. For physics this scale with its negative temperatures is not very appropriate, however, and it does not conform with Eq. (1). The kelvin scale in which one counts from absolute zero in steps of

$$1 \text{ K} = T_0 / 273.16, \quad (2)$$

where T_0 is the triple point of water, is a common choice for a thermodynamic temperature scale. The triple point, a state of water in which ice, liquid and vapour coexist in equilibrium, is chosen because it corresponds to a unique temperature and pressure of the system. The value 273.16 K is assigned to the triple point temperature in order to get the degree on kelvin scale as nearly equal as possible with the Celsius degree. Absolute zero can also be defined by a Carnot process. It proves that there is always a limit, thermodynamic temperature of zero, that cannot be attained by a finite work done by the system. [17,18]

For thermometers used in everyday applications there is typically no direct relation of the measured quantity with temperature. Thus, one has to calibrate such thermometers by a primary one. For primary thermometers our theoretical knowledge

about the measured property of matter is good enough to extract the thermodynamic temperature without calibration. A few fundamental physical laws that serve to define an absolute temperature scale have been discovered. They are absolute in the sense that they do not contain any sample-dependent parameters or any other constants that depend on any particular experiment. These laws are presented in the following sections dealing with the methods for low temperature thermometry.

An official international temperature scale is needed to provide a common basis for precise comparisons of measurements related to temperature. This has been done by establishing a number of fixed temperature points, and by using them to allow interpolation by certain thermometric methods in between. The most recent of these temperature scales is the International Temperature Scale of 1990. [19] The lower end of ITS-90 from 0.65 K to 5.0 K is defined by means of the vapour pressure of liquid ^3He and ^4He . At temperatures between 3.0 and 24.5561 K a constant-volume helium gas thermometer is used as a defining instrument. Electrical resistance of pure platinum is used for temperatures from 13.8033 to 1234.93 K. The Planck radiation law using monochromatic radiation is applied for the upper end of ITS-90. 17 fixed points, mostly phase transitions of pure substances, are chosen for calibration of the defining thermometers. The temperature scale is transferred from primary standard thermometers maintained by government agencies to secondary ones and further to working standards which are used to calibrate thermometers for the market. [20] The next international temperature scale will probably be extended to below 0.65 K. [21]

4.2 Cryogenic thermometers

In the following commonly used methods for low temperature thermometry are shortly presented. The physical principles, some typical features and measurement techniques are discussed. The basic information about these methods, except viscosity thermometry and CBT, is found in Refs. 16, 20, 22, 23, and 24. A review of the recent progress in thermometry between 0.3 K and 160 K is presented in Ref. 25.

4.2.1 Gas thermometry

The gas thermometer is a basic defining method of the temperature scale used since the 19th century. In principle, it is a primary thermometer based on the kinetic theory of gases. In the case of an ideal gas, if the system has n moles of gas in a volume V at a temperature T , the pressure is given by the equation of state, $pV = nRT$, where R is the gas constant. This equation defines the perfect gas temperature scale. For a real gas the interaction between molecules and the finite dimensions of them must be taken into account. The equation of state for real gases is

$$p = \frac{nRT}{V} \left[1 + B(T) \left(\frac{n}{V} \right) + C(T) \left(\frac{n}{V} \right)^2 + \dots \right], \quad (3)$$

where B and C are so called virial coefficients characteristic of each gas.

The measurement can be performed either at constant pressure or at constant volume. Temperatures in the ITS-90 are defined by a constant volume gas thermometer in the range 3.0 K to the triple point of Ne at 24.5561 K. Gas thermometry is complex in practice and one has to take into account the dead volumes of the system, thermal and elastic volume changes and absorption and desorption of gas from the container walls. High-precision gas thermometry is mostly supported by national laboratories for calibration purposes or to establish the temperature scale.

4.2.2 Vapour pressure thermometry

Measurement of vapour pressure above a cryogenic fluid is less complicated and more accurate than gas thermometry. It is a secondary method and has to be calibrated. In ITS-90, the vapour pressure of ³He and ⁴He is used to define the scale from 0.65 K to 5.0 K. The p - T relations for the helium isotopes are given in ITS-90.

In practice, the temperature over the liquid which determines the vapour pressure may be considerably different from the temperature lower down in the bath, although in superfluid ⁴He below about 2 K such gradients are absent. For more precise measurements one has to use a small vapour pressure cell connected to the

experiment. Thus, one needs a filling line for the cell and a capillary connecting the pressure gauge to the cell. This increases the complexity of the system, and also, the evaporation of the cryoliquid. The best precision is attained using a low temperature capacitive pressure transducer connected directly to the experiment. Helium vapour pressure thermometry is frequently used for the calibration of resistance thermometers.

4.2.3 Helium melting pressure thermometry

The melting temperature of ^3He is strongly dependent on pressure. This feature is utilised in melting curve thermometry which employs the p vs. T relation [26] by enclosing a mixture of liquid and solid ^3He in a cell that has one flexible wall. When the melting pressure changes as a result of a change in temperature this wall is displaced, and the corresponding change in capacitance between the flexible wall and a fixed electrode is detected.

The melting pressure curve also provides four fixed points: a minimum, two superfluid transition points and a magnetic phase transition in the solid, which can be used as fixed points either for temperature or pressure. The useful temperature range extends from 1 mK to about 1 K. The advantages of melting curve thermometry are the high resolution (about 1 μK) and reproducibility (several ppm) and essentially zero power dissipation. Drawbacks are the rather large specific heat of liquid ^3He in the thermometer, and the need of a substantial amount of ^3He and a high-pressure gas handling system with a fill capillary. The capacitance sensor must also be calibrated against a pressure standard. The melting pressure is slightly depressed by a magnetic field.

So far, the properties of ^3He are not known theoretically well enough to make melting pressure thermometry a primary method. There has been, however, discussion about extension of ITS-90 below 0.65 K by means of melting curve thermometry and several superconductive transition temperatures. [21]

4.2.4 Acoustic thermometry

Acoustic thermometry is a primary method closely related to the gas thermometry. The temperature dependent quantity is the speed of sound in a gas given by

$$v^2 = \frac{\gamma RT}{M} + A_1(T)p + A_2(T)p^2 + \dots, \quad (4)$$

where $\gamma = C_p/C_v$ is the ratio of heat capacities at constant pressure and volume, respectively, R is the gas constant, M is the molecular weight of the gas, and A_i are nonideality corrections for a real gas known as acoustic virial coefficients. They can be expressed in terms of the virial coefficients of Eq. (3). [23]

Acoustic thermometry has been used at temperatures between about 2 and 2500 K. A cylindrical or a spherical resonator is used to determine the wavelength of sound corresponding to a certain frequency or to determine the resonance frequency corresponding to the diameter of the sphere, respectively. A more recent attempt utilises a time interval between reflections in a tube consisting of two parts with different diameters. [27] This method, however, needs calibration at one temperature point.

4.2.5 Viscosity thermometry

The viscosity of liquid ^3He - ^4He has a known temperature dependence ($\eta \propto T^{-2}$) and it provides a secondary thermometer. Viscosity can be measured by a vibrating wire viscometer, which is a loop of thin wire immersed into liquid. The loop is vibrated by applying an alternating current through the wire in the presence of a magnetic field. Viscous damping of the resonance of the vibration is measured. The equipment needed for the measurement is an oscillator with a frequency sweep and a lock-in amplifier. Vibrating wire viscometer has been used to measure temperature of the He mixture in dilution refrigerators between $130 \mu\text{K} < T < 100 \text{ mK}$ with an

accuracy of a few per cent. [28, 29] Viscometer reading can be corrected to take into account the effect of magnetic fields.

4.2.6 Thermoelectricity

If the ends of a metallic wire are at different temperatures, a thermoelectric voltage will develop along the wire. In practice, the thermoelectric power $S = \Delta U / \Delta T$, where ΔU is the thermoelectric voltage and ΔT is the temperature difference between the ends of the wires, between two different metals is measured with a reference junction at a known temperature. Typically, the thermopower is several microvolts per kelvin for practical thermocouples, but it vanishes for $T \rightarrow 0$. Normally, without special techniques, the accuracy for thermocouple measurements is worse than 1 %. At low temperatures a superconductor with $S = 0$ is used as a reference wire and the very small thermoelectric voltages can be detected by a SQUID (superconducting quantum interference device). In this way a resolution of 1 μK at 1 K is possible with a Au-Fe thermocouple, which has a thermopower of $-9 \mu\text{V} / \text{K}$ at 1 K.

The sensor of a thermoelectric thermometer is considerably small, a wire junction, and it has a small specific heat. Also, the device and the measurement, which does not essentially produce heat input, are simple. A good reproducibility and moderate insensitivity to magnetic field (except for magnetic alloys that are used at temperatures below 10 K) are also advantages of thermoelectric thermometry. However, great care must be taken to avoid spurious thermoelectric voltages developing in other parts of the thermometer system: in the leads to room temperature, at soldering joints, switches and other contacts between different metals. These voltages are harmful especially at low temperatures where their effect may be even larger than the desired signal from the junction. Thermoelectric thermometry is best suited for measuring temperature differences above 10 K.

4.2.7 Resistance thermometry

Thermometry based on temperature-dependent electrical resistance of metals, semiconductors or carbon is probably the most widely used method of low-temperature thermometry. The resistivity has seldom a known temperature dependence, therefore resistance thermometers must be calibrated. Apart from this the temperature dependence is usually far from linear. Resistance thermometers are available with either positive (metals) or negative (semiconductors and carbon) temperature coefficients of resistance.

Platinum (Pt) is the most commonly used pure metal. As an interpolating method, platinum resistors define a wide range of ITS-90 (~14 K ... ~1000 K). The temperature dependence of resistance of Pt is quite linear down to 50 K but the sensitivity vanishes below 10 K, and this is the practical lower limit of the temperature range. The manufacture process of the platinum resistors is so controllable that the sensors are interchangeable above 70 K. A Pt thermometer is rather sensitive to magnetic field at temperatures below 30 K.

A resistor made of a dilute alloy of rhodium and iron has a temperature coefficient that is similar to that of Pt but larger at low temperatures. Rh-Fe resistors are useful down to about 0.5 K. They have been accepted for use as secondary temperature standards in many national standards laboratories. Rh-Fe resistance thermometers are not applicable for use in the presence of magnetic fields.

The temperature coefficient of semiconductors is negative or the resistance increases with decreasing temperature because of the decreasing number of charge carriers. At low temperatures very high sensitivities (and resistances) are common. Due to this extreme nonlinearity no simple calibration functions can be found.

The most widely used secondary thermometers are carbon resistors. Carbon resistors are typically not specially manufactured for thermometry but taken from the electronics industry. The best known commercial types are Allen-Bradley, Matsushita and Speer. None of these are produced anymore. Carbon resistors have been cheap and thus extensively used and are still being used as cryogenic temperature sensors. The temperature range extends down to about 10 mK. The stability of carbon resistors

is poor, and they should be calibrated in each run if accuracy of a few percent or better is desired. Due to the rather high heat capacity and low thermal conductivity their use in the millikelvin temperature range requires special care. Carbon thermometers show a magnetoresistance of typically a few percent per tesla.

Germanium doped with As or Ga is suited for thermometry at temperatures from about 50 mK to 100 K and above. Possibly the most advantageous feature of germanium thermometers is the good stability of their R - T relationship. A Ge sensor is recognised as a “secondary standard thermometer” for transferring temperature scales. Ge thermometers have a strong orientation-dependent magnetoresistance and they are not applicable for use in a magnetic field.

Carbon-glass resistors have been used especially in high magnetic field applications because of their small and predictable magnetic field dependence. Carbon-glass sensor is useful at temperatures down to about 1 K. The sensitivity and reproducibility are high at low temperatures but not above 100 K.

Thick-film chip resistors based on ruthenium oxide, normally used in microcircuits, have been found suitable for low temperature thermometry. Their advantages are the good reproducibility and sensitivity. RuO_2 resistors are applicable for temperatures from about 30 mK to 300 K and they show a magnetoresistance which increases with decreasing temperature being typically less than 1 %/T for Temperatures above 1 K.

Temperature sensors based on a thin film of zirconium oxynitride are commercially available under the name Cernox. [20] Their temperature range extends from 0.3 K to above room temperature. They have a sensitivity which is high at low temperatures and remains sufficient up to the room temperature. The magnetic field induced errors for the Cernox sensors are negligible at temperatures higher than 30 K and a few per cent at temperatures below 4 K at fields above 5 T. Thermal response time is faster than for bulk resistors. Presently this is one of the most popular among the commercial calibrated sensors.

Resistance temperature sensors are mostly measured by applying a small DC current through the sensor and detecting the resulting voltage across it. A four wire measurement is often needed in order to avoid errors due to the lead resistances. At

low temperatures the measurements have to be performed at very low power to prevent self heating of the sensor. A DC measurement is not applicable then. AC techniques enable lower measuring power and higher sensitivity and most importantly, eliminate the effect of thermal voltages. Resistance bridges for low temperature thermometry based on AC techniques are commercially widely available.

4.2.8 Diode thermometry

The junction voltage of a semiconductor diode biased at a constant current increases with decreasing temperature. Diode sensors with temperature range from 1.4 K to above room temperature are available. The most widely used diode thermometers are made of silicon junctions. Their temperature characteristics are highly predictable and stable. Si diodes show high magnetoresistance at low temperature. The disadvantage of magnetic field dependence is somewhat reduced in gallium-aluminium-arsenide diode sensors but it is still typically a few per cent at helium temperature for $B < 5$ T.

4.2.9 Capacitance thermometry

Some dielectric materials show changes of their dielectric constant with changing temperature. Capacitance measurement is relatively simple and produces insignificant heating. Capacitance temperature sensors have the advantage of being insensitive to magnetic field, but their reproducibility in thermal cycling is poor and they can drift in time even while at low temperatures. Therefore calibrated ones are not available. Capacitance thermometers based on SrTiO₃ glass ceramic are commercially available with a useful temperature range of 1 K – 290 K, but their use as thermometers has been demonstrated at much lower temperatures. They are best suited for use in temperature control.

4.2.10 Noise thermometry

Noise thermometry is a method which measures the thermal noise power spectrum of a resistor. The random thermal motion of the conduction electrons in a

metal results in temperature dependent voltage noise of a resistive element. Owing to the well-verified law relating noise to temperature it provides a primary thermometer. The root-mean-square noise voltage within the frequency band from ν to $\nu + d\nu$ of a resistance R is given by

$$\langle u^2(\nu) \rangle^{1/2} = (4Rk_B T d\nu)^{1/2}. \quad (5)$$

The major difficulty in using this method for accurate thermometry is the practical problem of measuring very small noise voltages, especially at low temperatures. The noise generated in amplifiers operated at room temperature can be equal or larger than the one to be measured. Naturally all the resistive elements of the measurement circuit are also noise sources.

These difficulties are diminished by incorporation of a SQUID as the amplifying element into the design of a noise thermometer. SQUID is used either as a preamplifier of the current generated by the noise voltage or as a voltage-to-frequency converter. Nevertheless, the rest of the equipment in the circuit is at temperatures between 4 K and 300 K. In addition, one has to determine the effective bandwidth of the electronics and the amplifying factor of the voltage measurement. The use of secondary noise thermometry is somewhat more straightforward. One can calibrate the system, e.g., by putting the resistor at a known temperature.

Typically, if an accuracy of 0.1 % in temperature is required, measuring time has to be several hours. This is quite a disadvantage for practical applications. Noise thermometry is mostly used by standards laboratories for calibration purposes at temperatures down to 10 mK.

4.2.11 Magnetic thermometry with electronic paramagnets

The magnetic susceptibility for paramagnetic materials is related to temperature. This relation is known as the Curie-Weiss law in which the susceptibility of a paramagnet has nearly an inverse dependence on temperature: $\chi \propto (T + A)^{-1}$. There are measurement-circuit parameters, as well as material dependent parameters that

must be calibrated by some other physical laws. Therefore magnetic thermometry is in practice a secondary method. The most frequently used paramagnetic salt has been cerium magnesium nitrate (CMN). Minimum temperatures down to a few mK and resolution and reproducibility of about 10^{-4} at temperatures $0.5 \text{ K} < T < 3 \text{ K}$ have been obtained by CMN thermometers. The ordering temperature of the magnetic moments determines the low-temperature limit of magnetic thermometry, which is about 1 mK for the electronic magnetic moments. The upper end of the temperature range is usually limited to about 1 K due to the loss in sensitivity.

The change in susceptibility can be detected by measuring the mutual inductance of coils where a sample of a paramagnetic salt is placed in one of the coils forming an astatic pair. The magnetic moments are oriented by a static magnetic field generated by another coil surrounding the sample. AC mutual inductance bridges suitable for this measurement are commercially available. The sensitivity can be enhanced by using a SQUID as the detecting element.

Advantages of magnetic thermometry are the relatively simple and quick measurement, simple temperature dependence of the susceptibility, high sensitivity at low temperatures, and minor heating due to the measurement. A drawback is the complexity of the sample and coils, and size, normally several cm^3 , of the sensor. Particular care must be taken in order to avoid magnetic materials near the thermometer. Susceptibility thermometer has to be properly protected against magnetic fields. Even with a careful shielding the use of magnetic thermometry in an external magnetic field is limited. Critical field of niobium, which is commonly used as a shield material, is about 0.2 T.

4.2.12 Nuclear magnetic thermometry

Nuclear magnetic thermometry is based on the Curie law between magnetic susceptibility of nuclei and temperature, $\chi \propto T^{-1}$. Temperature range extends from about 0.1 K down to a few microkelvin due to the low ordering temperature of the nuclear magnetic moments. In nuclear magnetic thermometry one can use pure metals

which give better thermal conductivity and contact and faster thermal response time than paramagnetic salts.

The most commonly used method is nuclear magnetic resonance (NMR) techniques on ^{195}Pt . There are two ways to perform NMR thermometry. In the continuous wave method magnetic field applied to the sample is swept and transitions between the nuclear energy levels induced by a RF magnetic field are detected. Another way is to use short pulses of RF field. By NMR techniques one can also measure the temperature of electrons T_e by measuring the spin-lattice relaxation time τ_1 and applying the Korringa law $\tau_1 T_e = \kappa$, where κ is a material constant. NMR thermometry is most commonly used at temperatures below 1 mK.

4.2.13 Nuclear orientation thermometry

Anisotropy of emission of gamma rays has a well known temperature dependence. The intensity of γ -radiation from nuclei oriented by a magnetic field is measured. The angular distribution is given by

$$W(\theta, T) = 1 + \sum_{k=1} B_k(T) R_k P_k(\cos\theta), \quad (6)$$

The temperature information is included in

$$B_k(T) \propto \frac{\exp(-E_m/k_B T)}{\sum_m \exp(-E_m/k_B T)}, \quad (7)$$

where E_m are the energies of the nuclear states. All the details of the decay scheme must be determined first by other measurements. [30]

Nuclear orientation is a primary thermometric method because the theory is well established and no extra calibration is needed. The sensitivity is limited to a certain temperature range whose mean value depends on the isotope used and it is usually

between 3 and 50 mK. The two most commonly used isotopes are ^{60}Co and ^{54}Mn because all the necessary decay parameters are known for them. The nuclei must be oriented by a magnetic field which can be applied externally or by implanting the radioactive isotope into a ferromagnetic host matrix. The measuring equipment consists of a γ -ray detector, a preamplifier, and a multichannel analyser with a PC.

An advantage of nuclear orientation thermometry is that metal can be used to ensure thermal contact to the point whose temperature is to be measured. No leads at all are needed to the sample because only the emitted γ -rays are measured. Nuclear orientation thermometry is a statistical method and thus one needs a certain counting time to obtain the desired accuracy. Typically this is several minutes, because the activity of the source has to be low in order to avoid self-heating. Any external magnetic field is obviously harmful because it changes the orientation of the nuclei. Also, the γ -ray detectors are usually sensitive to magnetic field. Nuclear orientation method is often applied for calibration purposes, and most commonly in a $^3\text{He}/^4\text{He}$ dilution refrigerator.

4.2.14 CBT thermometry

The most recent candidate for primary thermometry is Coulomb blockade thermometer (CBT), the main topic of this thesis, based on electron tunneling of electrons in nanoscale tunnel junction arrays. It was invented and it has been further developed at the Physics Department of University of Jyväskylä. [P1 - P8, P10, 31, 32] The temperature information is included in the conductance characteristics of the junction array. The differential conductance (dI/dV) vs. bias voltage curve has a minimum around zero bias whose width is directly proportional to temperature. The full width at half minimum, $V_{1/2}$, and the temperature are related by

$$eV_{1/2} = 5.439Nk_B T, \quad (7)$$

where e is the electron charge, N is the number of junctions in the array, k_B is the Boltzmann constant, and the numerical factor 5.439... originates from the universal shape of the conductance minimum. Linear temperature dependence gives constant sensitivity over the whole temperature range. A small linear correction must be applied to Eq. (7) due to the nonzero depth of the minimum. The conductance curve gives also another temperature dependent parameter; the depth of the minimum is inversely proportional to temperature. This can be calibrated with the absolute parameter, $V_{1/2}$, and used as a secondary thermometer. Thus, CBT can be operated in two modes.

Useful temperature range extends from 20 mK to about 30 K. The temperature range is adjustable by fabrication parameters and by choosing suitable mean temperatures the whole range, 0.02 K – 30 K, can be covered by two sensors. The sensor is a tiny small thin film structure on a silicon substrate consisting of several parallel connected tunnel junction arrays. Thermal response time of such a device is short and in practice it is limited by the properties of the substrate and encapsulation materials.

Measurement is done by applying a DC voltage sweep across the sensor and detecting the response of small AC excitation current added to the bias. Sensors are fairly resistive, typically 100 k Ω , and the half width measurement is immune to thermoelectricity in the circuit and to changes in lead resistances. Therefore even single-ended measurement is adequate. A four probe measurement would be necessary only for high precision measurements where an accuracy in temperature of better than 10^{-3} is desired. The lead resistance changes etc. can impair the reliability of the secondary temperature signal, but by frequent calibration with the primary measurement this effect can be minimised.

CBT has been found immune to magnetic field at least at temperatures 0.4 – 4.2 K up to 23 T. CBT thermometry provides the first primary method that is suitable for everyday use in cryogenic applications.

4.3 Summary

The useful temperature ranges of the cryogenic thermometers are collected in Table 1. They are not the ultimate limits, but more practical ranges found in Refs. 16, 20, 22, 23, 27, 28, 29, and 33. One also has to take into account that the whole temperature range is not always covered by one sensor.

Table 2 shows some important properties of the cryogenic thermometers discussed. The relation between the measured quantity and temperature is shown in the second column for primary thermometers in (a). For secondary ones in Table 2 (b) the form of the temperature dependence is presented. In the third column of both tables the performance of the thermometer in the presence of magnetic field at cryogenic temperatures is evaluated as follows:

Excellent ↔ No magnetic field dependence observed

Good ↔ Very small and/or predictable magnetic field dependence

Moderate ↔ Small and/or predictable magnetic field dependence in most of the temperature range

Poor ↔ Strong, not predictable magnetic field dependence or measurement technique disturbed by magnetic field

In the last column some special features and the best suited applications are collected.

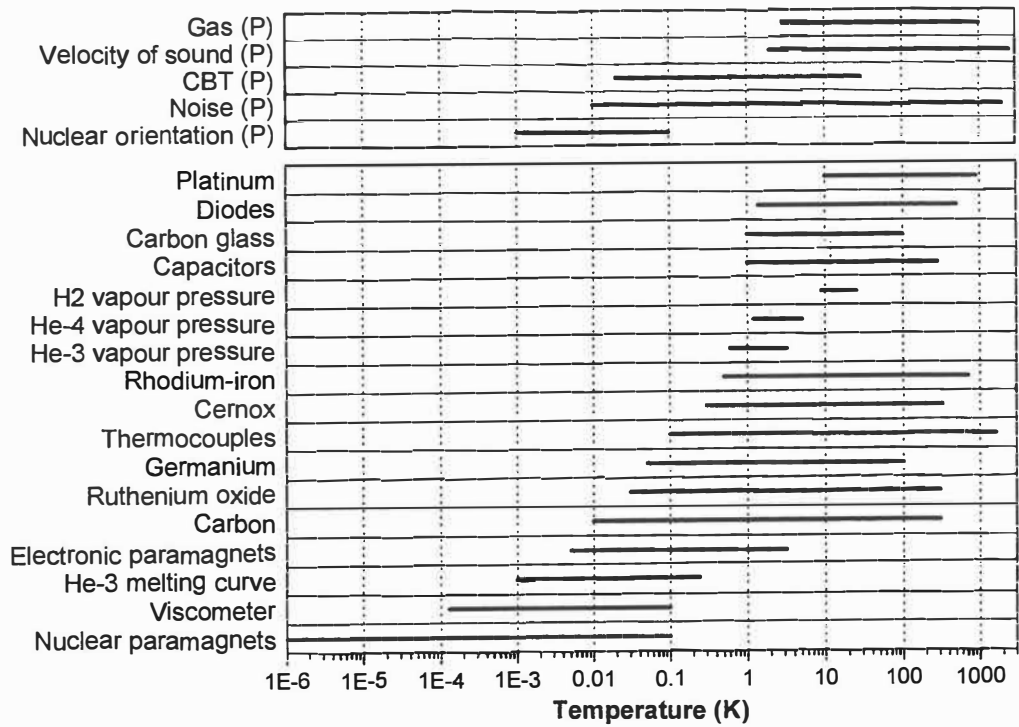


Table 1. Temperature ranges of selected cryogenic thermometers (P ↔ primary).

Primary thermometer	Temperature law	Performance in magnetic field	Suitable application
Gas	$pV = nRT$	Excellent	Calibrations
Nuclear orientation	$W = f(E_m/k_B T)$	Poor	Calibrations
Noise	$\langle u^2(\nu) \rangle_t = 4Rk_B T d\nu$?	Calibrations
Speed of sound	$v^2 = \gamma RT/M$?	Calibrations
CBT	$eV_{1/2} = 5.439Nk_B T$	Excellent	Normal lab. use / calibrations

(a)

Secondary thermometers	Temperature dependence	Performance in magnetic field	Notes, (typical use)
Vapour pressure	$\exp[\Sigma a_i T^i]$	Excellent	High resolution, ITS-90
³ He melting curve	$\Sigma a_i T^i$	Good	High resolution and stability
Viscometer	T^{-2}	Good	No thermal contact problems
Resistors			Simple measurement
Platinum	$\Sigma a_i T^i$	Moderate	Interchangeable, ITS-90
Rhodium-iron	$\Sigma a_i T^i$	Poor	Good stability
Carbon	$\exp[\Sigma a_i (\ln T)^i]$	Poor	Cheap, high sensitivity at low T
Germanium	$\exp[\Sigma a_i (\ln T)^i]$	Poor	Stable, high sensitivity at low T
Ruthenium oxide	$\exp[\Sigma a_i (\ln T)^i]$	Moderate	Cheap, good stability
Carbon-glass	$\exp[\Sigma a_i (\ln T)^i]$	Good	High sensitivity at low T
Cernox	$\exp[f(T)]$	Good	Thin film sensor, good stability
Capacitors		Excellent	High resolution, (T -control)
Diodes		Poor	Small sensor, interchangeable
Thermoelectricity	$\Sigma a_i T^i$	Moderate	Tiny sensor, (ΔT measurements)
Electronic susceptibility	T^{-1}	Poor	Simple measurement
Nuclear susceptibility	T^{-1}	Poor	extensively used at $T < 1$ mK

(b)

Table 2. Temperature dependence, magnetic field tolerance, and some other features of the cryogenic primary thermometers in (a) and secondary thermometers in (b).

5. Publications

- [P1] J.P. Pekola, K.P. Hirvi, J.P. Kauppinen, and M.A. Paalanen, *Thermometry by arrays of tunnel junctions*, Phys. Rev. Lett. **73**, 2903 (1994).
<https://doi.org/10.1103/PhysRevLett.73.2903>

For the first time, we showed that arrays of tunnel junctions between normal metal electrodes exhibit features suitable for primary thermometry. I - V and dI/dV characteristics were calculated for two junctions including a universal analytic high temperature result. Experimentally we showed that in this regime the width of the conductance minimum scales with T and N , the number of junctions. Its value agreed with the calculated one to within 3 % for large N . The depth of the conductance minimum at zero bias was shown to be inversely proportional to T .

- [P2] K.P. Hirvi, J.P. Kauppinen, A.N. Korotkov, M.A. Paalanen, and J.P. Pekola, *Arrays of normal metal tunnel junctions in weak Coulomb blockade regime*, Appl. Phys. Lett. **67**, 2096 (1995).
<https://doi.org/10.1063/1.115090>

Thermometric features of the tunnel junction arrays were tested against inhomogeneities in the junction parameters, number of junctions in the array, and magnetic field. Thermometer arrays were found tolerant to fabrication inhomogeneities and independent of magnetic field up to 8 T with 2 % of reproducibility of the measurements. The electromagnetic environment of the arrays affects the performance of short arrays.

- [P3] J.P. Kauppinen and J.P. Pekola, *Electron-phonon heat transport in Al islands of arrays with submicron size tunnel junctions*, Phys. Rev. B **54**, R8353 (1996).
<https://doi.org/10.1103/physrevb.54.r8353>

We presented experimental evidence of the effect of electrode volume and its shape on thermalisation of tunnel junction arrays with micrometer-size islands. The power

law and the magnitude of the thermal transport was investigated. We found that it obeys the common T^5 law for electron-phonon coupling only for the smallest islands studied. In other cases considered, with extra cooling fins attached to the islands, the coupling is weaker and it rather follows a power law with an exponent < 5 .

[P4] J.P. Kauppinen and J.P. Pekola, *Charging in Solitary, Voltage biased Tunnel Junctions*, Phys. Rev. Lett. **77**, 3889 (1996).
<https://doi.org/10.1103/PhysRevLett.77.3889>

We presented experiments and a phenomenological model on the zero bias anomaly of a single, voltage biased tunnel junction. The conclusion was that this resistance peak is determined purely by the charging effect, and this result is in agreement with the observation of end effects in thermometry by short arrays in [II].

[P5] Sh. Farhangfar, K.P. Hirvi, J.P. Kauppinen, J.P. Pekola, J.J. Toppari, D.V. Averin, and A.N. Korotkov, *One dimensional arrays and solitary tunnel junctions in the weak Coulomb blockade regime: CBT thermometry*, J. Low Temp. Phys. **108**, 191 (1997).
<https://doi.org/10.1007/BF02396821>

This is a review article on the use of tunnel junction arrays for primary thermometry. Important new results are the low temperature corrections to the half width and depth of the conductance dip beyond the linear approximation. We also pointed out that short arrays show interesting deviations from the universal behaviour of the long arrays.

[P6] T.A. Knuuttila, K.K. Nummila, W. Yao, J.P. Kauppinen, and J.P. Pekola, *Direct measurements of electron thermalization in Coulomb blockade nano-thermometers at millikelvin temperatures*, Physica E, in press (1998).
[https://doi.org/10.1016/S1386-9477\(98\)00207-0](https://doi.org/10.1016/S1386-9477(98)00207-0)

We investigated electron thermalization of tunnel junction arrays installed in a powerful dilution refrigerator whose mixing chamber can produce lattice temperatures

down to 3 mK. We were able to detect and discriminate between the heat load delivered through the wiring and that produced by the bias current of the measurement. We demonstrated that by careful anchoring of the leads and design of the sample equilibrium temperature of 20 mK can be achieved by Coulomb blockade thermometry.

- [P7] J.P. Pekola, J.J. Toppari, J.P. Kauppinen, K.M. Kinnunen, A.J. Manninen, and A.G.M. Jansen, *Coulomb Blockade-based Nanothermometry in Strong Magnetic Fields*, *J. Appl. Phys.* **83**, 5582 (1998).
<https://doi.org/10.1063/1.367397>

The performance of Coulomb blockade thermometry in strong magnetic fields was tested up to 23 T at temperatures of 0.4 – 4.2 K. We confirmed that to within the accuracy of about ± 1 % the temperature parameters were unaffected by the application of magnetic field. A simple theoretical basis was discussed. Also, we reported on the practical limitation at low temperatures imposed by superconductivity of aluminium in small magnetic fields.

- [P8] J.P. Kauppinen and J.P. Pekola, *Coulomb blockade nanothermometer*, *Microelectronic Engineering* **41/42**, 503 (1998).
[https://doi.org/10.1016/S0167-9317\(98\)00117-8](https://doi.org/10.1016/S0167-9317(98)00117-8)

This is a proceedings article of the Micro- and nanoengineering conference MNE 97 in which we presented an overview of CBT thermometry and the first results of neutron irradiation hardness of the sensors.

- [P9] J.P. Pekola and J.P. Kauppinen, *Insertable dilution refrigerator for characterization of mesoscopic samples*, *Cryogenics* **34**, 843 (1994).
[https://doi.org/10.1016/0011-2275\(94\)90072-8](https://doi.org/10.1016/0011-2275(94)90072-8)

We describe a small ^3He - ^4He dilution refrigerator which can be inserted into a helium transport Dewar. Dilution inserts made of plastic and metal were tested. The unit was found practical for fast and economical measurements down to 50 mK.

[P10] J.P. Kauppinen, K.T. Loberg, A.J. Manninen, J.P. Pekola, and R.A. Voutilainen, *Coulomb Blockade Thermometer: Tests and Instrumentation*, Rev. Sci. Instrum., submitted (1998).
<https://doi.org/10.1063/1.1149265>

We review the principles and the operation of CBT, and present new data about radiation hardness and stability of the sensors. We describe the instrumentation of CBT in detail. We have developed two signal conditioning units for CBT measurements. One is an extended AC resistance bridge, a versatile laboratory instrument operating with a PC computer, and the other is a simple stand-alone instrument for direct temperature reading.

6. The author's contribution

I have taken part in the measurements and data analysis in [P1] and [P7]. I have done most of the sample fabrication, measurements and data analysis in [P5] and [P2]. This work was entirely done by me in [P3] and [P4]. In [P6] I have taken part in the planning and realisation of the experimental setup and sample fabrication. I have taken part in the construction and cooling tests of the dilution refrigerator in [P9]. Such refrigerators have been used in all the measurements at temperatures below 4.2 K carried out in Jyväskylä. Article [P8] is entirely, and [P10] is mostly written by me. I have been actively working for the development of the CBT sensor and the signal conditioning units, and I carried out the irradiation tests.

7. References

- [1] G.-L. Ingold and Yu. V. Nazarov, in *Single Charge Tunneling, Coulomb Blockade Phenomena in Nanostructures*, edited by H. Grabert and M.H. Devoret, Plenum Press, New York, 1992.
- [2] D.V. Averin and K.K. Likharev, in *Mesoscopic Phenomena in Solids*, edited by B.L. Altshuler, P.A. Lee, and R.A. Webb, Elsevier, Amsterdam, 1992.
- [3] H.J. Levinson and W. H. Arnold, in *Handbook of Microlithography, Micromachining, and Microfabrication*, edited by P. Rai-Choudhury, p. 121, SPIE, Bellingham, 1997.
- [4] T.A. Fulton and G.J. Dolan, *Phys. Rev. Lett.* **59**, 109 (1987).
- [5] C.I.M. Beenakker and S.K. Bootsma, in *Frontiers in Nanoscale Science of Micron/Submicron Devices*, edited by A.-P. Jauho and E.V. Buzaneva, Kluwer Academic Publishers, Dordrecht, 1996.
- [6] S. Altmeyer, A. Hamidi, B. Spangenberg, and H. Kurz, *J. Appl. Phys.* **81**, 8118 (1997).
- [7] W. Chen and H. Ahmed, *J. Vac. Sci. Technol. B* **13**, 2883 (1995).
- [8] E. Leobandung, L. Guo, and S.Y. Chou, *Appl. Phys. Lett.* **67**, 2338 (1995).
- [9] H. Ishikuro and T. Hiramoto, *Appl. Phys. Lett.* **71**, 3691 (1997).
- [10] K. Matsumoto, M. Ishii, K. Segawa, Y. Oka, B.J. Vartanian, and J.S. Harris, *Appl. Phys. Lett.* **68**, 34 (1996).
- [11] E.S. Snow, D. Park, and P.M. Campbell, *Appl. Phys. Lett.* **69**, 269 (1996).
- [12] S. Tiwari, F. Rana, H. Hanafi, A. Hartstein, E.F. Crabbé, and K. Chan, *Appl. Phys. Lett.* **68**, 1377 (1996).
- [13] L. Guo, E. Leobandung, and S.Y. Chou, *Appl. Phys. Lett.* **70**, 850 (1997).
- [14] A. Nakajima, T. Futatsugi, K. Kosemura, T. Fukano, and N. Yokoyama, *Appl. Phys. Lett.* **70**, 1742 (1997).
- [15] *Micro- and Nano-engineering 97*, Proceedings of the International Conference on Micro- and Nanofabrication, Elsevier, Amsterdam, 1997.

- [16] F. Pobell, *Matter and Methods at Low Temperatures*, 2nd edition, Springer, Berlin, 1996.
- [17] F.W. Sears, *An Introduction to Thermodynamics, the Kinetic Theory of Gases, and Statistical Mechanics*, 2nd edition, Addison-Wesley, Reading, 1965.
- [18] F. Mandl, *Statistical Physics*, 2nd edition, Wiley, Essex, 1989.
- [19] H. Preston-Thomas, *Metrologia* **27**, 3 (1990).
- [20] Lake Shore Cryotronics, Inc., Ohio.
- [21] R.J. Soulen, Jr and W.E. Fogle, *Physics Today*, August 1997.
- [22] Oxford Instruments, Research Instruments, UK.
- [23] T.J. Quinn, *Temperature*, 2nd edition, Academic Press, 1990.
- [24] R.P. Hudson, H. Marshak, R.J. Soulen, Jr, and D.B. Utton, *J. Low Temp. Phys.* **20**, 1 (1975).
- [25] L.G. Rubin, *Cryogenics* **37**, 341 (1997).
- [26] D.S. Greywall, *Phys. Rev. B* **33**, 7520 (1984).
- [27] H. Ziegler and M. Spieker, *Proceedings of TEMPMEKO '96, 6th International Symposium on Temperature and Thermal Measurements in Industry and Science*, Levrotto & Bella, Torino, 1997.
- [28] D.I. Bradley and R. Oswald, *J. Low Temp. Phys.* **80**, 89 (1990).
- [29] R. König, A. Betat, and F. Pobell, *J. Low Temp. Phys.* **97**, 311 (1994).
- [30] H. Marshak, *Journal of Research of the National Bureau of Standards*, Vol. 88, No. 3, p. 175 (1983).
- [31] K.P. Hirvi, J.P. Kauppinen, M.A. Paalanen, and J.P. Pekola, *J. Low Temp. Phys.* **101**, 17 (1995).
- [32] K.P. Hirvi and J.P. Pekola, *Comp. Phys. Commun.* **106**, 69 (1997).
- [33] P.V.E. Mc Clintock, D.J. Meredith, and J.K. Wigmore, *Matter at Low Temperatures*, Wiley, New York, 1984.